Cell PRESS
Neuron
Article

TNFα Controls Glutamatergic Gliotransmission in the Hippocampal Dentate Gyrus

Mirko Santello,[1] Paola Bezzi,[1] and Andrea Volterra[1,*]
[1]Department of Cell Biology and Morphology, University of Lausanne, Rue du Bugnon 9, 1005 Lausanne, Switzerland
*Correspondence: andrea.volterra@unil.ch
DOI 10.1016/j.neuron.2011.02.003

SUMMARY

Glutamatergic gliotransmission provides a stimulatory input to excitatory synapses in the hippocampal dentate gyrus. Here, we show that tumor necrosis factor-alpha (TNFα) critically controls this process. With constitutive TNFα present, activation of astrocyte P2Y1 receptors induces localized $[Ca^{2+}]_i$ elevations followed by glutamate release and presynaptic NMDA receptor-dependent synaptic potentiation. In preparations lacking TNFα, astrocytes respond with identical $[Ca^{2+}]_i$ elevations but fail to induce neuromodulation. We find that TNFα specifically controls the glutamate release step of gliotransmission. In cultured astrocytes lacking TNFα glutamate exocytosis is dramatically slowed down due to altered vesicle docking. Addition of low picomolar TNFα promptly reconstitutes both normal exocytosis in culture and gliotransmission in situ. Alternatively, gliotransmission can be re-established without adding TNFα, by limiting glutamate uptake, which compensates slower release. These findings demonstrate that gliotransmission and its synaptic effects are controlled not only by astrocyte $[Ca^{2+}]_i$ elevations but also by permissive/homeostatic factors like TNFα.

INTRODUCTION

There are several indications that glial cells participate in the physiological control of synaptic transmission and plasticity via the release of synaptically effective mediators, a process called gliotransmission (reviewed in Perea et al., 2009; Volterra and Meldolesi, 2005; see also Henneberger et al., 2010). However, some studies fail to see synaptic regulation by glia and question the physiological relevance of gliotransmission (Agulhon et al., 2010; Fiacco et al., 2007; Petravicz et al., 2008). We identified a positive astrocytic control at perforant path (PP)-granule cell (GC) synapses in the hippocampal dentate gyrus (Jourdain et al., 2007). Firing of PP afferents triggers intracellular Ca^{2+} ($[Ca^{2+}]_i$) elevations in nearby astrocytes of the dentate molecular layer (ML). Astrocytes respond robustly to trains of evoked action potentials, but are also activated by sparse endogenous PP firing activity occurring in the slices in the absence of external stimulation. Intriguingly, part of the synaptically evoked astrocytic $[Ca^{2+}]_i$ elevations are mediated by purinergic P2Y1 receptors (P2Y1R), which in the ML are expressed predominantly, if not exclusively, in astrocytes, notably in the processes surrounding excitatory synapses (Jourdain et al., 2007). As a consequence of P2Y1R-dependent $[Ca^{2+}]_i$ elevation, glutamate is released from astrocytes via a mechanism which is sensitive to blockers of neuronal exocytosis (Domercq et al., 2006) and induces potentiation of excitatory transmission at PP-GC synapses. This glial glutamatergic control operates under physiological conditions, as its blockade reduces basal EPSC activity in GCs evoked by endogenous PP firing (Jourdain et al., 2007) and is mediated by a presynaptic mechanism involving stimulation of NR2B-containing NMDA receptors (NMDAR). Indeed, both functional and ultrastructural evidence indicates that such receptors are located presynaptically, in the extrasynaptic portion of excitatory nerve terminals making synapses onto GCs (Jourdain et al., 2007); for a review on presynaptic NMDAR (pre-NMDAR) see Corlew et al. (2008). Interestingly, we found that presynaptic NR2B subunits generally face perisynaptic astrocytic processes containing groups of small vesicular organelles (synaptic-like microvesicles, SLMV; Bezzi et al., 2004; Jourdain et al., 2007). In immunogold experiments, astrocytic SLMV were shown to contain glutamate and express proteins for uptake and release of the amino acid, including vesicular glutamate transporters (VGLUT) and the v-SNARE protein, VAMP3/cellubrevin (Bezzi et al., 2004; Jourdain et al., 2007). In spite of this ultrastructural information, the modalities and the regulation of astrocytic glutamate release in situ remain largely undefined. Moreover, contradictory results on the capacity of astrocytic $[Ca^{2+}]_i$ elevations to trigger glutamatergic gliotransmission at CA3-CA1 synapses (Agulhon et al., 2010; Fellin et al., 2004; Fiacco et al., 2007; Henneberger et al., 2010; Perea and Araque, 2007) suggest that the process may have specific Ca^{2+} requirements or even that additional unknown regulatory factors are involved (Hamilton and Attwell, 2010; Kirchhoff, 2010; Shigetomi et al., 2008; Tritsch and Bergles, 2007). In this context, we reported that the cytokine TNFα exerts a potent control on P2Y1R-evoked Ca^{2+}-dependent glutamate exocytosis in cultured astrocytes (Domercq et al., 2006). Measures of glutamate release with a specific assay (Bezzi et al., 1998; Nicholls et al., 1987) detected a dramatic reduction of the P2Y1R-evoked release in astrocyte cultures lacking TNFα signaling. The mechanism by which TNFα achieves this effect and the relevance of the TNFα-dependent control to the astrocyte-dependent synaptic potentiation in situ are unknown. TNFα is mostly regarded as a "proinflammatory" cytokine, produced by and acting in the brain in response to infection,

injury, or disease (Gosselin and Rivest, 2007; Wetherington et al., 2008). However, TNFα is expressed also in the normal brain, albeit at much lower levels than during inflammatory reactions, and participates in homeostatic brain functions (Boulanger, 2009; Vitkovic et al., 2000). In particular, constitutive TNFα has recently been implicated in control of the stability of neuronal networks in response to prolonged changes in activity via the phenomenon of synaptic scaling (Stellwagen and Malenka, 2006; Turrigiano, 2008) and plays a specific role in ocular dominance plasticity upon monocular visual deprivation (Kaneko et al., 2008). The cytokine, released from astrocytes, was reported to strengthen excitatory synaptic transmission by promoting surface insertion of AMPA receptor (AMPAR) subunits (Bains and Oliet, 2007; Beattie et al., 2002; Stellwagen et al., 2005). In the present study, we find that TNFα is also an obligatory factor for the induction of synaptically effective gliotransmission at GC synapses in the dentate gyrus, specifically controlling glutamate release from astrocytes. Notably, constitutive levels of the cytokine promote functional docking and rapid coordinated secretion of glutamatergic vesicles in cultured astrocytes. Indeed, TNFα most likely determines the kinetics of P2Y1R-dependent glutamate release in situ and the local extracellular concentration of the amino acid, a critical factor in the activation of pre-NMDAR and, ultimately, in the potentiation of GC synapses.

RESULTS

P2Y1R-Evoked Gliotransmission Increases mEPSC Activity in GC via Pre-NMDAR

To investigate the role of TNFα in astrocyte-dependent synaptic modulation in hippocampal dentate gyrus, we planned studies on *Tnf*$^{-/-}$ mice (Pasparakis et al., 1996). Our previous work in rats established that purinergic P2Y1R, strongly expressed in astrocytic processes around GC synapses, respond to stimulation with the agonist 2-methylthioadenosine-5′-diphosphate (2MeSADP, 10 μM) by inducing a highly reproducible increase in mEPSC frequency in GCs (Jourdain et al., 2007). We therefore decided to utilize this stimulus paradigm and recorded mEPSCs from hippocampal dentate GCs in acute mouse hemibrain horizontal slices from P18–P23 mice. Recordings were performed 50–90 μm deep in the slices, where astrocytes and the patched GCs retained their integral tridimensional structures, as confirmed by two-photon imaging of cells fluorescently labeled with specific markers (Figure 1A). Initially, we used slices from wild-type (WT) mice and applied 2MeSADP either by bath perfusion or locally, within the volume of the recorded GC, via pressure ejection from a micropipette. In both cases the P2Y1R agonist increased mEPSC frequency in GCs (bath application: +37% ± 11%; $p < 0.05$; n = 14 cells; local application: +32% ± 10%, $p < 0.05$; n = 7 cells), with no effect on the amplitude or kinetics of the currents (Figure 1B and see Figure S1 available online). The effect of the drug on mEPSC frequency was abolished in the presence of N6-methyl-2′-deoxyadenosine-3′,5′-bisphosphate (MRS2179 10 μM; n = 7 cells), a P2Y1R blocker, confirming the specific involvement of this purinergic receptor subtype. MRS2179 per se had no effect on basal mEPSC frequency (Figure 1C). In order to verify the obligatory role of astrocyte $[Ca^{2+}]_i$ elevation in the 2MeSADP synaptic effect, we repeated P2Y1R stimulations upon intracellular dialysis of the Ca^{2+} chelator 1,2-bis(2-aminophenoxy) ethane-N,N,N′,N′-tetra-acetic acid (BAPTA, 10 mM) selectively into the astrocytes (Figure 1D). This treatment prevents $[Ca^{2+}]_i$ rise in several gap-junction-connected astrocytes surrounding the synapses on the dendritic arbor of the patched GC (Jourdain et al., 2007). In this situation, 2MeSADP never induced an increase in mEPSC frequency (n = 8 cells; Figure 1E). Finally, the 2MeSADP-evoked effect was found to depend on NMDAR activation. Thus, the increase in mEPSC frequency was abolished in the presence of ifenprodil (3 μM), a selective NR2B-containing NMDAR antagonist that per se had no effect on basal mEPSC frequency (n = 10 cells; Figure 1F). In conclusion, these experiments show that (1) P2Y1R activation induces, in mice, a gliotransmission cascade and synaptic effect on GCs similar to those previously observed in rats (Jourdain et al., 2007); (2) this astrocytic modulatory pathway is not endogenously activated by TTX-independent spontaneous synaptic release events at GC synapses, as indicated by the fact that neither MRS2179, nor BAPTA, nor ifenprodil affected basal mEPSC frequency.

Gliotransmission Loses Synaptic Efficacy in the Absence of Constitutive TNFα

Next, we addressed the role of constitutive TNFα in astrocyte-evoked synaptic modulation, by testing the effect of 2MeSADP stimulation in slices from *Tnf*$^{-/-}$ mice. In basal conditions, frequency and amplitude of the mEPSC events in GCs were comparable to those observed in WT mice (Figure S2; Kaneko et al., 2008; Stellwagen and Malenka, 2006). However, application of 2MeSADP failed to produce the expected increase in mEPSC frequency (+5% ± 13%; n = 8 cells; Figure 2A), suggesting that the presence of TNFα is necessary for astrocytic P2Y1R-evoked synaptic modulation. To confirm that the defect observed in *Tnf*$^{-/-}$ mice is specifically due to the absence of the cytokine, we preincubated *Tnf*$^{-/-}$ slices with low picomolar concentrations of recombinant TNFα (60–150 pM). In this condition, while basal mEPSC frequency did not change (*Tnf*$^{-/-}$: 1.62 ± 0.26 Hz, n = 29 cells; *Tnf*$^{-/-}$ + TNFα: 1.64 ± 0.19 Hz; n = 13 cells), 2MeSADP application induced a selective increase in the number of mEPSC events, similar to its effect in WT slices (Figure 2B; +51% ± 22%; $p < 0.05$; n = 13 cells). Interestingly, in initial experiments we used prolonged TNFα preincubations (1–4 hr), but we then found that 15 min in the presence of the cytokine were sufficient to reconstitute the 2MeSADP effect. Preincubation of *Tnf*$^{-/-}$ slices with TNFα produced a second type of effect, on the amplitude of the mEPSC events, which was slightly but significantly increased in basal condition (*Tnf*$^{-/-}$: 6.07 ± 0.26 pA, n = 29 cells; *Tnf*$^{-/-}$ + TNFα: 7.87 ± 0.52 pA; $p < 0.05$; n = 13 cells), but not further modified by 2MeSADP application. This P2Y1R-independent effect is strongly reminiscent of the effect ascribed to the control of AMPAR trafficking by TNFα in WT mice (Stellwagen et al., 2005; Stellwagen and Malenka, 2006). In a final set of experiments, we tested whether constitutive levels of endogenous TNFα control P2Y1R-dependent synaptic modulation in WT slices. To this end, we preincubated the slices with a scavenger for the cytokine, the soluble form of TNF receptor (sTNFR,

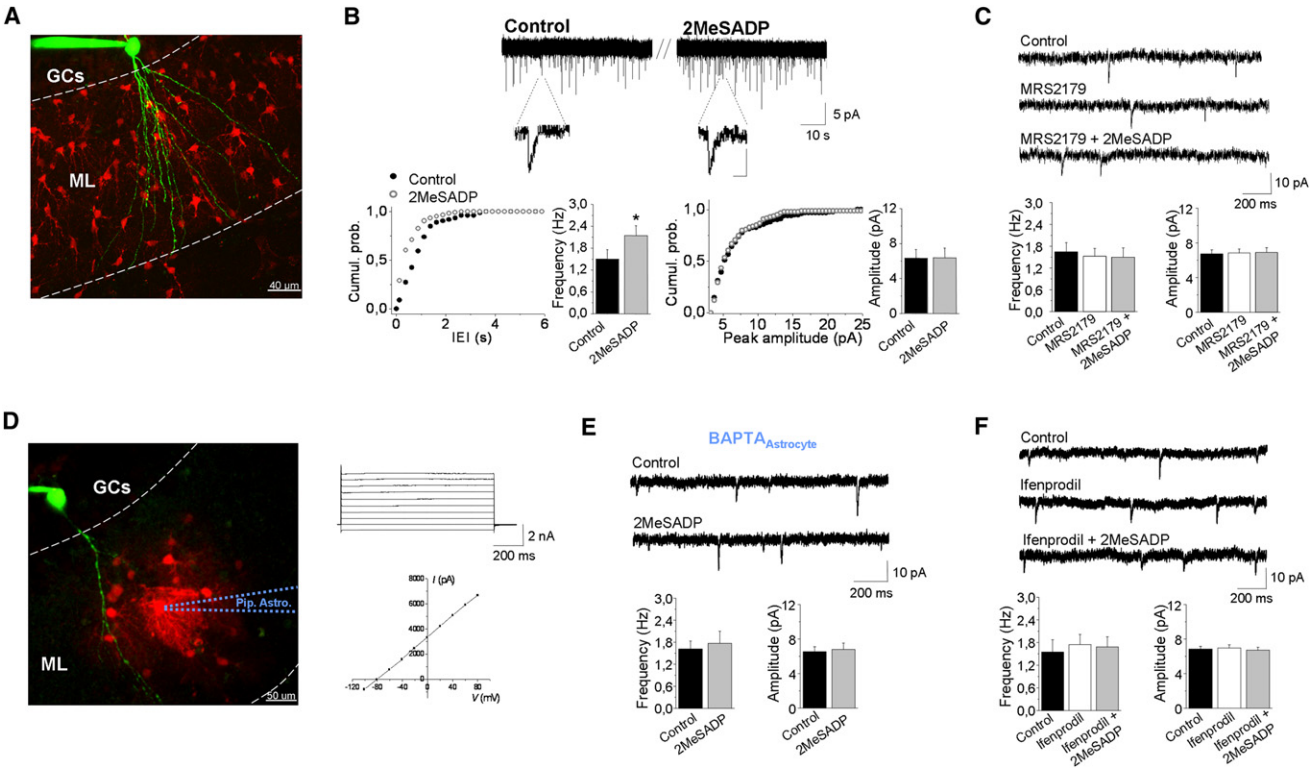

Figure 1. Astrocyte P2Y1R-Dependent Activation of Presynaptic NMDAR Increases Synaptic Release Probability

(A) Example of whole-cell patch-clamp recording of a hippocampal granule cell (GC, green, Alexa 488) contacting with the dendritic arborization multiple molecular layer (ML) astrocytes stained with SR-101 (red), as observed 80 μm deep in the slice with two-photon microscopy (z stack: 100 μm).

(B) Top: representative whole-cell recording of mEPSC activity in a granule cell (−65 mV). Control: basal condition; 2MeSADP: bath application of the purinergic P2Y1R agonist, 2MeSADP (10 μM). Insets: representative mEPSC events for each condition (scale: 5 ms, 5 pA). Bottom: cumulative probability plots of the same experiment comparing mEPSC inter-event interval (IEI) and amplitude before (control, black dots) and during P2Y1R stimulation (2MeSADP, gray open dots). Plots are accompanied by histograms of mean mEPSC frequency and amplitude (n = 14 GCs). Noteworthy, in 10/14 GCs, 2MeSADP selectively increased mEPSC frequency (+ 50% ± 11%, $p < 0.001$), whereas in 4 it was without effect.

(C) Top: mEPSC currents in a representative recording from a hippocampal GC during: the control period, bath application of the specific P2Y1R antagonist MRS2179 (10 μM), and subsequent application of 2MeSADP (10 μM) in the presence of MRS2179. In 7/7 tested GCs, 2MeSADP, in the presence of MRS2179, failed to increase mEPSC frequency. Bottom: histograms of mean values of frequency and amplitude in the three conditions. No statistical difference was detected.

(D) Left: two-photon image showing a single astrocyte whole-cell clamped with an internal solution containing 10 mM BAPTA and the low molecular weight fluorophore, Alexa 594 (100 μM, red) and patch-clamp recording from a GC neuron filled with Alexa 488. After removal of the pipette, a number of astrocytes gap-junction-coupled to the patched one are dialyzed with the BAPTA-containing solution (19 in the shown example). Right: electrophysiological identification of a "passive astrocyte" displaying linear I/V curve in response to 20 mV depolarizing steps from –100 mV to +80 mV.

(E) Top: representative traces of mEPSC activity recorded from a hippocampal GC after dialysis of the astrocytic syncytium with BAPTA (see Experimental Procedures for details on the protocol of these experiments and the controls performed). Application of 2MeSADP in these conditions does not produce any variation in the frequency or amplitude of the events. Bottom: histograms representing the corresponding mean values obtained from 8 recorded GCs. No statistical differences were detected.

(F) Top: representative traces of mEPSC activity recorded from a GC during the control period, bath application of ifenprodil (3 μM), or of 2MeSADP (10 μM) in the presence of ifenprodil. Bottom: histograms show no variations in mean frequency or amplitude of mEPSCs in the presence of ifenprodil or of 2MeSADP + ifenprodil (n = 10 GCs). Statistics: one-way ANOVA + Scheffé test for multiple comparisons and paired t test; Error bars: SEM.

See also Figure S1.

15 μg/ml). This manipulation, while not changing basal mEPSC activity (frequency: 1.70 ± 0.21 Hz; amplitude 6.49 ± 0.41 pA; n = 9 cells), fully prevented the stimulatory effect of 2MeSADP on mEPSC frequency (+6% ± 10%; n = 9 cells; Figure 2C). Overall, these data demonstrate that constitutive levels of TNFα are necessary for effective P2Y1R-dependent gliotransmission at PP-GC synapses and call for an understanding of the underlying mechanism.

TNFα Does Not Control P2Y1R-Dependent $[Ca^{2+}]_i$ Elevations in Astrocytic Processes

Several steps of the P2Y1R-dependent stimulus-secretion coupling in astrocytes could be the target of a tonic control by TNFα. At first we investigated GPCR-dependent signal-transduction leading to astrocyte $[Ca^{2+}]_i$ elevation. Importantly, we have recently observed that the $[Ca^{2+}]_i$ elevations responsible for the physiological P2Y1R-dependent control of presynaptic

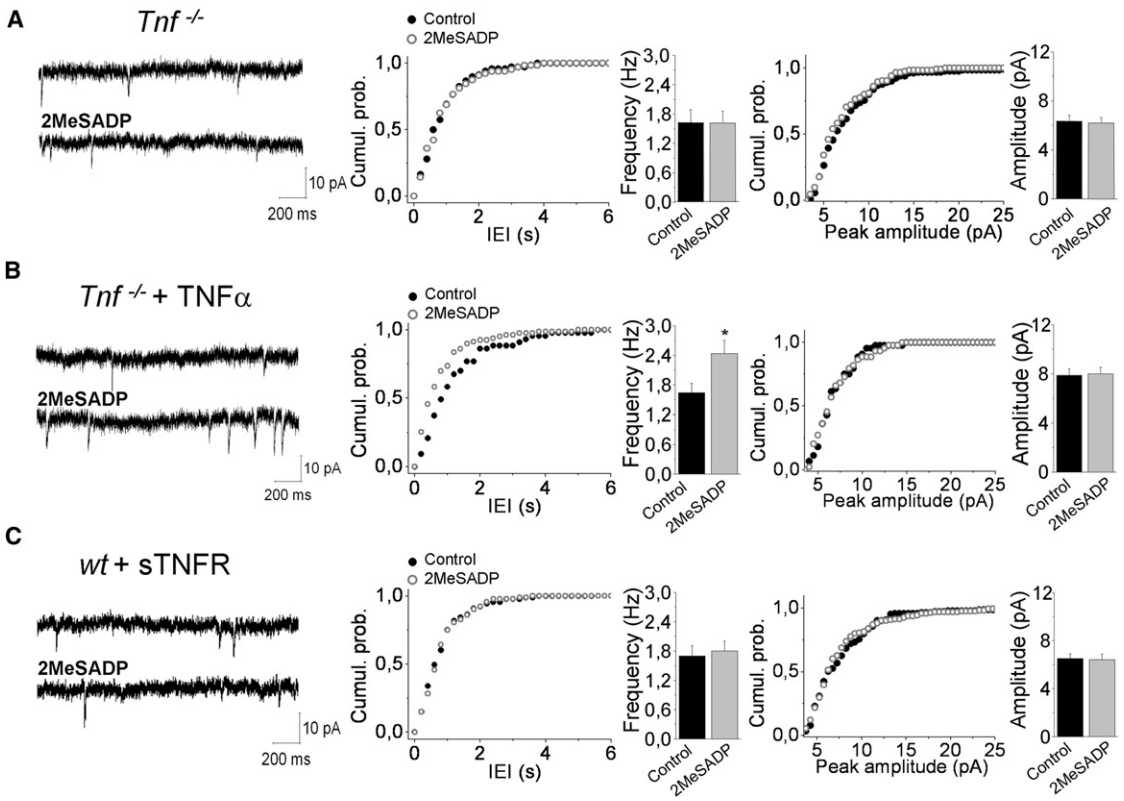

Figure 2. Astrocyte-Mediated Presynaptic Modulation Requires TNFα

(A) Experiments in slices from *Tnf*$^{-/-}$ mice. Left: 2MeSADP application induced no change in mEPSC activity in a GC. Right: corresponding cumulative distribution plots of mean mEPSC IEI and amplitude accompanied by histograms of mean mEPSC frequency and amplitude showing no effect of P2Y1R stimulation in 8 *Tnf*$^{-/-}$ GCs.

(B) Experiments in *Tnf*$^{-/-}$ slices preincubated with 60–150 pM TNFα for periods ranging from 15 min to 4 hr. As shown by traces, cumulative plots and histograms, 2MeSADP selectively increased mEPSC frequency in GCs if TNFα was preadded to the *Tnf*$^{-/-}$ slices (n = 13 cells). The effect was observed in 10/13 cells (+65% ± 27%, $p < 0.01$), whereas 3 did not respond to the drug. *$p < 0.05$, paired t test.

(C) Left, mEPSCs recordings from a WT slice where TNFα has been scavenged by sTNFR (1.5–2 hr, 15 μg/ml). P2Y1R stimulation in this condition does not modify synaptic activity. Right, cumulative distribution plots and histograms for mEPSCs frequency and amplitude average values before and upon 2MeSADP stimulation is slices incubated with sTNFR (n = 9). Statistics: unpaired t test; Error bars: SEM.

See also Figure S2.

excitatory function occur locally in astrocytic processes apposed to PP-GC synapses (Chuquet et al., 2010). We therefore specifically studied P2Y1R-evoked Ca^{2+} signaling in astrocytic processes with two-photon microscopy and compared local Ca^{2+} responses to agonist stimulation in WT and *Tnf*$^{-/-}$ slices. Experiments were performed on individual passive dentate ML astrocytes (see also Figure 1D for electrophysiological profile) dialyzed with a solution containing a Ca^{2+} indicator (Fluo-4 pentapotassium, 200 μM) and a Ca^{2+}-insensitive morphological dye (Texas Red dextran 3000, TxR, 150 μM; Figure 3A). Local Ca^{2+} activity in individual astrocytic processes, expressed as ΔG/R, was analyzed upon extracting the process of interest from the rest of the TxR image and subdividing it in many contiguous subregions (SRs) of similar area (9.2 ± 0.83 μm^2; Figure 3A) by use of a custom-made program (see details in Experimental Procedures). Appropriate conditions for focal P2Y1R stimulation were set by controlling duration (5 ms), pressure (4 psi) and distance of delivery (3–8 μm) of 2MeSADP (10 μM) puffs from a pipette positioned in the vicinity of the monitored astrocytic process. In WT slices, this protocol of focal 2MeSADP application produced fast $[Ca^{2+}]_i$ elevations (Figures 3B and 3C), seen immediately after the stimulus (average time to peak: 0.82 ± 0.15 s, n = 10; Figure 3E), that were spatially restrained to a few micrometers (on average 8.6 ± 0.9 μm^2; range 5–16 μm^2; n = 10) in the astrocytic process, normally corresponding to an individual SR. In a few cases, the signal also invaded contiguous SRs (range 27–55 μm^2; WT: n = 3). The specificity of these localized Ca^{2+} events was confirmed by the fact that (1) identical puffs of buffer solution did not evoke any $[Ca^{2+}]_i$ elevation (n = 3); (2) 2MeSADP-induced events were abolished in the presence of the P2Y1R antagonist MRS2179 and restored upon its washout (Figure 3D). The characteristics of 2MeSADP-evoked events, including their fast kinetics (Figure 3E), are consistent with those of the P2Y1R-dependent events evoked in astrocyte processes by endogenous synaptic activity (Chuquet et al., 2010). Importantly, when we repeated the experiments in *Tnf*$^{-/-}$ astrocytes, we could not

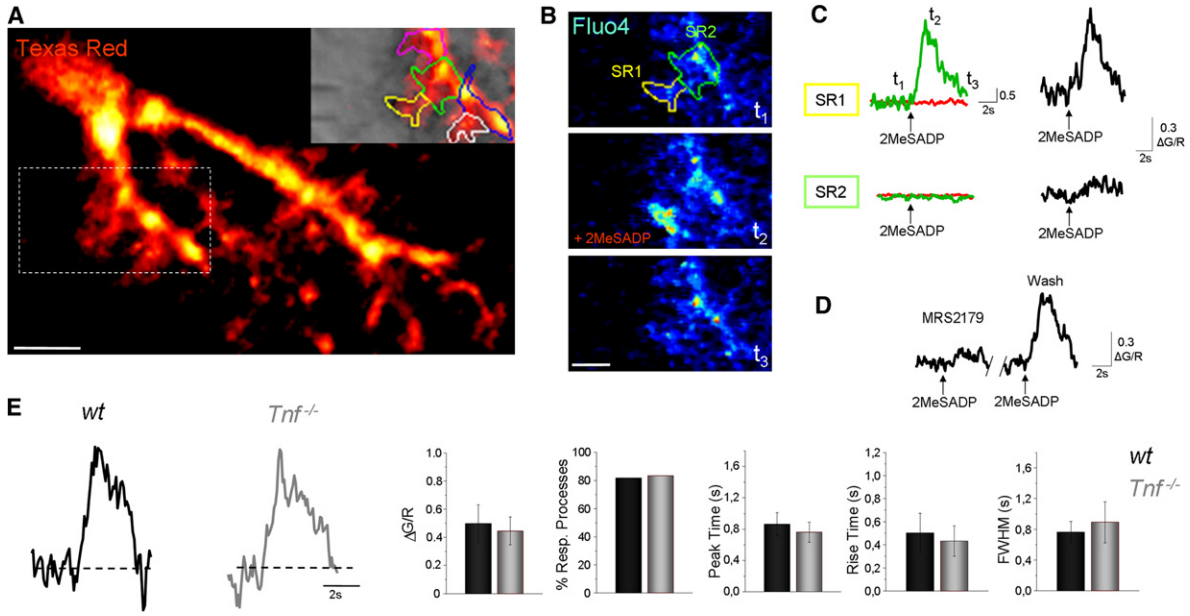

Figure 3. Absence of TNFα Does Not Perturb Local P2Y1R-Evoked Ca^{2+} Transients in Perisynaptic Astrocyte Processes

(A) Six micrometer Z stack projection of two major processes from a whole-cell patch-clamped astrocyte loaded with the morphological dye Texas Red Dextran 3000 (Texas Red) and Fluo4 pentapotassium (not visible) and imaged at 890 nm excitation wavelength. Scale bar: 10 μm. Inset: overlap of Texas Red fluorescence (red channel, average of 450 frames, excitation 810 nm) with "Dodt contrast" acquisition, the former revealing process structure, the latter position of the ejection pipette, ~6 μm away from the recorded process. The averaged Texas Red image was then used for morphological segmentation of the process into subregions of interest (colored lines).

(B) Fluo4 $[Ca^{2+}]_i$ elevation (green channel, here in pseudocolor) detected with 810 nm excitation wavelength upon brief focal 2MeSADP puff (10 μM, 5 ms, 4 psi). Images represent the $[Ca^{2+}]_i$ transient before, immediately after (2MeSADP), and 6 s after agonist application. Scale bar: 5 μm.

(C) Left, green (Fluo-4) and red (Texas Red) channel signals from subregions 1 and 2 (SR1, SR2) upon 2MeSADP stimulation. Notice that the red channel does not show any fluorescence variation, ruling out movement artifacts of the imaged process in response to the puff protocol. Right, $[Ca^{2+}]_i$ variations expressed as green channel signal normalized by the red channel signal (ΔG/R). Arrows represent time of 2MeSADP puff.

(D) $[Ca^{2+}]_i$ responses evoked by a 2MeSADP puff (arrows) in the presence of the specific P2Y1R antagonist MRS2179 and after its wash out.

(E) Left: average traces of $[Ca^{2+}]_i$ transients in WT and *Tnf*$^{-/-}$ slices, obtained by including responses from all the experiments. Traces are normalized to facilitate comparison of kinetics in the two preparations. Right: histograms show comparatively several parameters of 2MeSADP-evoked $[Ca^{2+}]_i$ transients in recordings from WT (n = 10) and *Tnf*$^{-/-}$ (n = 9) slices: average amplitude (ΔG/R), percentage of responding processes (% Resp. Processes) upon agonist stimulation, time between stimulus and maximal amplitude of the transient (peak time), 10–90 rise time, and duration at half width of maximum (FWHM). Error bars: SEM.

find any significant difference in the Ca^{2+} responses to 2MeSADP puffs with respect to WT astrocytes in any of the parameters analyzed, including percentage of responding processes, delay of the responses, their amplitude, and kinetics (Figure 3E; WT: n = 10, *Tnf*$^{-/-}$: n = 9). These results show that TNFα does not control P2Y1R-dependent $[Ca^{2+}]_i$ elevations in astrocytic processes. Hence, lack of synaptic efficacy in *Tnf*$^{-/-}$ slices cannot be directly ascribed to a defect in the P2Y1R-dependent Ca^{2+} signaling underlying stimulus-secretion coupling in astrocytes.

TNFα Controls Docking and Speed of Exocytosis of Glutamate Vesicles in Cultured Astrocytes

We therefore went on to investigate whether TNFα acts downstream to P2Y1R-evoked $[Ca^{2+}]_i$ elevations, in the Ca^{2+} dependent process leading to glutamate release from astrocytes. We initially turned to studies in cell cultures, where P2Y1R activation has been established to trigger glutamate release via vesicular exocytosis (Bowser and Khakh, 2007; Domercq et al., 2006) and where the underlying cellular events can be studied directly (Bezzi et al., 2004; Marchaland et al., 2008; Shigetomi et al., 2010). To this end, we used total internal reflection fluorescence (TIRF) microscopy and a specific marker of glutamatergic vesicle exocytosis, VGLUT1pHluorin, the chimerical fluorescent protein formed by vesicular glutamate transporter-1 (VGLUT1) coupled to pHluorin (Balaji and Ryan, 2007; Marchaland et al., 2008; Voglmaier et al., 2006). Even before studying the dynamics of P2Y1R-evoked exocytosis, we noticed a clear difference between WT and *Tnf*$^{-/-}$ astrocytes, in the number of VGLUT1-pHluorin-expressing vesicles present in the submembrane TIRF field, the so-called "resident" vesicles, thought to be docked to the plasma membrane (Marchaland et al., 2008; Zenisek et al., 2000). Thus, in *Tnf*$^{-/-}$ cells, "resident" vesicles, visualized by rapid alkalinizing NH_4Cl pulses (Balaji and Ryan, 2007), were about 50% less numerous than in WT cells (WT: 0.67 ± 0.08 vesicles/μm^2; n = 8 cells; *Tnf*$^{-/-}$: 0.35 ± 0.02 vesicles/μm^2; n = 16 cells; $p < 0.001$; Figure 4A). This defect was not due to a reduced overall number of glutamatergic vesicles in *Tnf*$^{-/-}$ astrocytes because the total VGLUT1-pHluorin fluorescence/cell under epifluorescence illumination was identical in *Tnf*$^{-/-}$ and WT

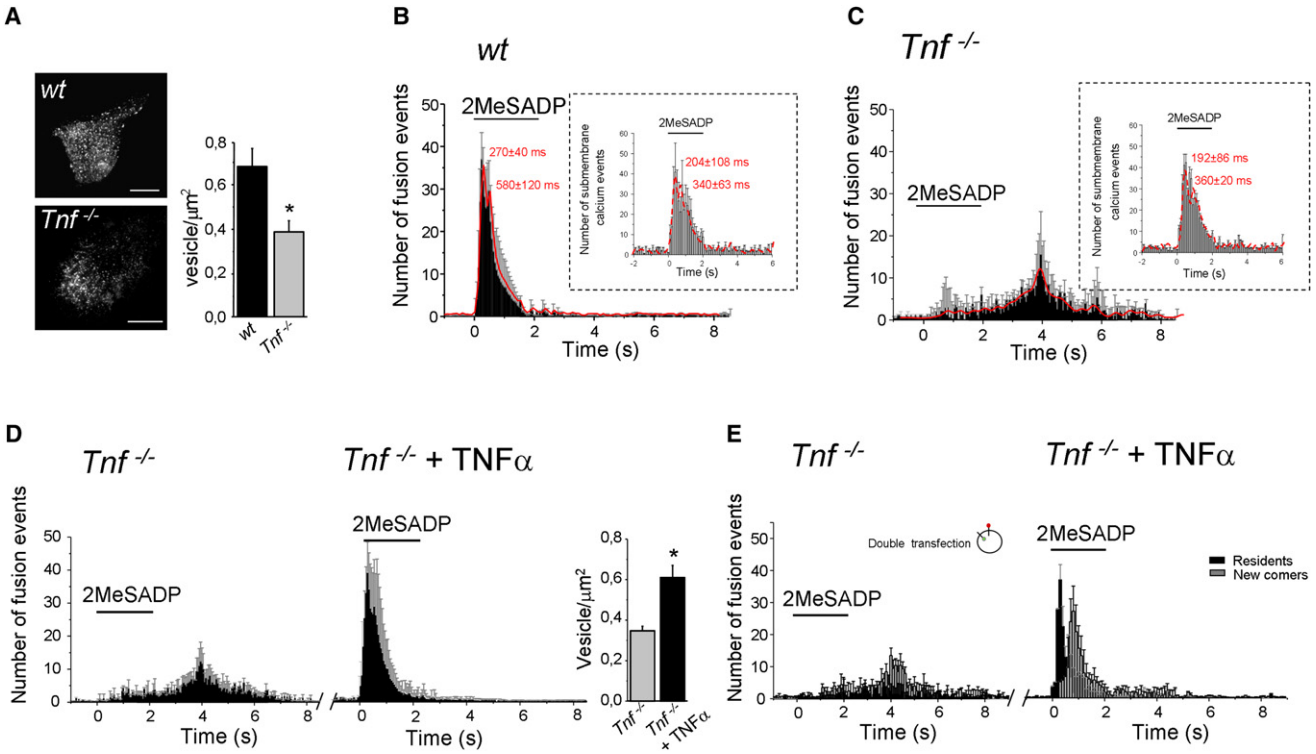

Figure 4. TNFα Is Necessary for Efficient Functional Docking and Rapid Synchronous Exocytosis in Cultured Astrocytes

(A) TIRF images showing "resident" VGLUT1-pHluorin-expressing vesicles in WT and *Tnf*$^{-/-}$ astrocytes in basal condition. Scale bar, 2 μm. Histograms represent the number of "resident" vesicle/area counted in the TIRF illumination field. This number is lower in *Tnf*$^{-/-}$ versus WT astrocytes (n = 16 and 8 cells, respectively; *p < 0.05: unpaired t test).

(B) Temporal distributions of fusion events of VGLUT1pHluorin vesicles and of submembrane Ca^{2+} events (in the insets) in response to 2MeSADP application (2 s, 10 μM). In WT astrocytes 2MeSADP evokes a biphasic burst of exocytosis (n = 12 cells; red: polynomial fit and peaks time). Each individual histogram represents the mean number (±SD) of fusion events detected in a 50 ms long frame. Inset: local stimulation with 2MeSADP (10 μM, 2 s) evokes submembrane Ca^{2+} events. The frequency of such Ca^{2+} events, low in basal conditions (0.33 ± 0.13/s/ROI, n = 34 cells for WT), increased by about 13-fold within the first 300 ms from the stimulus (4.5 ± 0.16/s/ROI) and the temporal distributions showed a biphasic burst in all similar to the one observed for the exocytic events, besides that Ca^{2+} peaks preceded exocytosis peaks.

(C) In *Tnf*$^{-/-}$ astrocytes 2MeSADP evokes slow, desynchronized exocytosis (n = 20 cells). Individual histograms and errors are as in (B). Inset: like in (B, inset) 2MeSADP evokes submembrane Ca^{2+} events: notice that the frequency (basal conditions: 0.33 ± 0.16/s/ROI; 300 ms after the stimulus: 3.75 ± 1.6/s/ROI, n = 29 cells) and the temporal distribution of Ca^{2+} events is identical to the one observed in WT astrocytes, but completely dissociated from that of exocytic events in *Tnf*$^{-/-}$.

(D) Temporal distributions of fusion events evoked in *Tnf*$^{-/-}$ astrocytes by two subsequent 2MeSADP pulses (interval: 3–8 min) applied before and after incubation with 30 pM TNFα (n = 7 cells). Left: before TNFα astrocytes respond to 2MeSADP with desynchronized exocytosis. Center: upon TNFα incubation, the 2MeSADP-evoked biphasic burst of exocytosis is reconstituted. Each histogram represents the mean number (±SD) of fusion events counted in a 50 ms long frame. Right: histograms show that addition of TNFα (30 pM) to *Tnf*$^{-/-}$astrocytes without 2MeSADP stimulation induces a statistically significant increase in the number of "resident" vesicles; *p < 0.05: unpaired t test.

(E) Temporal distribution of fusion events in *Tnf*$^{-/-}$ astrocytes doubly transfected with the VGLUT1pHluorin (green) and VGLUT1mCherry (red) constructs, before (left) and after (right) TNFα incubation. Black histograms: "resident" vesicles; gray histograms: "newcomer" vesicles. Notice that in the absence of TNFα, and similar to (D), the two rapid phases of the burst were abolished (30 ± 9.2 events/s during the stimulus) and the fusion events reached a small peak around 4 s. There was no temporal segregation between events attributable to "resident" and "newcomer" vesicles. When *Tnf*$^{-/-}$ astrocytes were preincubated with TNFα (30 pM, 3–8 min), the exocytic response was reconverted to a rapid biphasic burst like in WT cultures (181.6 ± 60 events/s during the stimulus; first peak: 200–300 ms; second peak: 400–600 ms; n = 7 cells) and fusions of "residents" (first peak) preceded those of "newcomers" (second peak). Each histogram represents the mean number (±SD) of fusion events counted in a 100 ms long frame.

See also Figure S3.

astrocytes (WT: 156.24 ± 17; n = 8 cells; *Tnf*$^{-/-}$ 152.12 ± 7.5; n = 16 cells). Next, we studied evoked exocytosis in WT and *Tnf*$^{-/-}$ cells by stimulating P2Y1R with 2MeSADP (10 μM, 2 s). Figure 4B shows that, in WT astrocytes, 2MeSADP produced a biphasic burst of exocytic events (456 ± 85; n = 12 cells) with the first peak occurring at ~270 ms from the start of the stimulus and the second one at ~580 ms. The number of fusion events, rare before the stimulus (4 ± 2 events/s), increased dramatically upon 2MeSADP application (198 ± 89.4 events/s during the stimulus) and returned to basal level in about 3 s. In *Tnf*$^{-/-}$ astrocytes, the effect observed was profoundly different (Figure 4C). Based on our previous glutamate release measures (Domercq et al., 2006), we expected to see a decreased number of exocytic events. In contrast, to our surprise, P2Y1R activation evoked the

same number of events as in WT astrocytes (504 ± 74; n = 20 cells). However, their temporal distribution was completely different, highlighting a dramatic slowing-down and desynchronization of the release process. No rapid biphasic burst was observed, just a small peak of fusion events that occurred at 3.8–4.2 s, i.e., more than 10-fold slower than the initial peak in WT astrocytes. In fact, the majority of the fusion events occurred sparsely in time (33.8 ± 23.8 events/s during the stimulus) and over a prolonged (8 s) period. Noteworthy, this dramatic temporal alteration was not just a peculiarity of P2Y1R-evoked glutamate exocytosis, because when we tested the effect of stromal cell-derived factor-1α (SDF-1α/CXCL12, 3 nM), a chemokine CXCR4 receptor agonist known to induce glutamate release from astrocytes (Bezzi et al., 2001; Calì et al., 2008), the agent not only evoked in WT astrocytes an exocytosis process with temporal characteristics analogs to the 2MeSADP-evoked process, but also produced in *Tnf*$^{-/-}$ astrocytes the same pattern of temporally altered fusions seen with the P2Y1R agonist (Figures S3A and S3B). That such temporal alterations depend specifically on the absence of constitutive TNFα was demonstrated by experiments in which we stimulated *Tnf*$^{-/-}$ astrocytes with 2MeSADP twice, first in the absence of TNFα and then after preincubating the cells with the cytokine (30 pM, 3–8 min). Figure 4D shows that addition of TNFα converted the slow and desynchronized response to the P2Y1R agonist into a rapid biphasic exocytic burst with events' distribution similar to that seen in WT cultures (550 ± 72 fusion events; 239.2 ± 76 events/s during the stimulus; first peak: ~260 ms; second peak: ~510 ms; n = 7 cells). In parallel control experiments, in which TNFα was not added between the first and second 2MeSADP pulse, the P2Y1R agonist produced twice the same slow response (Figure S3C). Interestingly, incubation of *Tnf*$^{-/-}$ astrocytes with TNFα had an additional effect, i.e., it increased the number of "resident" vesicles in basal condition, restoring the levels seen in WT astrocytes (Figure 4D, insets), suggesting that this basal defect and the one observed when evoking secretion may both depend on loss of the same TNFα-dependent regulatory mechanism. We therefore devised experiments to better understand such a mechanism. By doubly transfecting glutamatergic vesicles with a marker of the vesicle membrane (VGLUT1mCherry) together with VGLUT1pHluorin, we could distinguish two vesicular pools undergoing exocytosis upon P2Y1R stimulation: the "resident" pool (vesicles present in the TIRF field before the stimulus, in principle docked) and the "newcomers" pool (vesicles whose mCherry signal appeared in the TIRF field after the stimulus, which represent undocked vesicles arriving from the cytosol [Marchaland et al., 2008; Zenisek et al., 2000]). In WT astrocytes (data not shown) and in *Tnf*$^{-/-}$ astrocytes incubated with TNFα, (Figure 4E) the two pools underwent exocytosis in a clear biphasic temporal sequence: during the first phase (0–400 ms) most of the fusing vesicles belonged to the "resident" pool (80.6%, n = 7 cells), whereas during the second phase (500 ms–2 s), to the "newcomers" pool (82.5%). This temporal segregation reflects the different readiness to fusion of the two pools, in particular the fact that most "resident" vesicles, contrary to "newcomers," have already undergone the docking steps and are ready for fusion (i.e., are functionally docked [Ohara-Imaizumi et al., 2007; Toonen et al., 2006]). However, in *Tnf*$^{-/-}$ astrocytes, the situation was very different. Events attributable to "residents" decreased in percentage (20% instead of 40%; n = 3680 vesicle fusions analyzed, n = 7 cells). Moreover, importantly, events due to "residents" and "newcomers" occurred randomly, without the expected temporal segregation. This indicates that even the residual "resident" pool seen in Figure 4A is defective in *Tnf*$^{-/-}$ astrocytes, because it is not ready/competent to fuse. Most likely, these vesicles dock only transiently and, like all the others, in the absence of TNFα are hampered in reaching the stage of functional docking allowing them to undergo rapid fusion (Toonen et al., 2006). We conclude that constitutive TNFα is necessary for the correct reception of glutamatergic vesicles to release sites, a precondition for efficient exocytosis upon stimulation.

In parallel TIRF experiments, we studied local submembrane Ca^{2+} events, previously shown to be temporally locked to exocytic events (Marchaland et al., 2008). Indeed, in WT astrocytes, 2MeSADP stimulation induced a burst of submembrane Ca^{2+} events whose temporal pattern mirrored the one of VGLUT1-pHluorin fusion events, with two peaks of Ca^{2+} events, each one slightly preceding the corresponding peak of vesicular fusions (Figure 4B, inset). Importantly, and in full agreement with the observations in situ, this pattern was totally preserved in *Tnf*$^{-/-}$ astrocytes (Figure 4C, inset), further confirming that TNFα does not act on the coupling between GPCR and $[Ca^{2+}]_i$ elevation, and indicating that this step of gliotransmission can be perfectly normal while the downstream signaling is dramatically defective.

Lack of TNFα Shifts the Dynamic Competition between Astrocyte Glutamate Release and Uptake

The above results, indicating a tonic control of TNFα on P2Y1R-evoked astrocyte glutamate release, seem at odds with two previous observations that (1) TNFα itself induces glutamate release from astrocytes (Bezzi et al., 2001; Rossi et al., 2005) and (2) P2Y1R-evoked glutamate release is strongly reduced in *Tnf*$^{-/-}$ preparations (Domercq et al., 2006). The first point is explained by dose dependency of the TNFα effects (Figure 5A). Indeed, when tested at the concentration used in our previous studies (1.8 nM), the cytokine induced exocytic fusion of VGLUT1pHluorin-expressing vesicles. However, this direct effect was observed only at TNFα concentrations ≥300 pM, 10-fold higher than the concentration reconstituting normal P2Y1R-evoked exocytosis in cultured *Tnf*$^{-/-}$ astrocytes. The second point is explained by competition between release and uptake of glutamate from astrocytes, which causes reduced detection of the P2Y1R-evoked glutamate release in *Tnf*$^{-/-}$ preparations (Figure 5B). This competition was revealed by comparing 2MeSADP-evoked release in the presence and absence of the uptake blocker, DL-*threo*-beta-benzyloxyaspartate (TBOA). Like in previous studies, we measured glutamate in *Tnf*$^{-/-}$ cultures by adding the metabolic enzyme glutamic dehydrogenase (GDH) to the medium (Bezzi et al., 2004; Nicholls et al., 1987). TBOA was then added at a concentration (25 μM) not affecting the basal glutamate level. In spite of this, TBOA profoundly affected detection of P2Y1R-evoked glutamate release which, in its presence, was increased by ~10-fold (from 0.058 ± 0.008 to 0.56 ± 0.1 nmol/mg prot; n = 5 and 7; $p < 0.05$ unpaired t test)

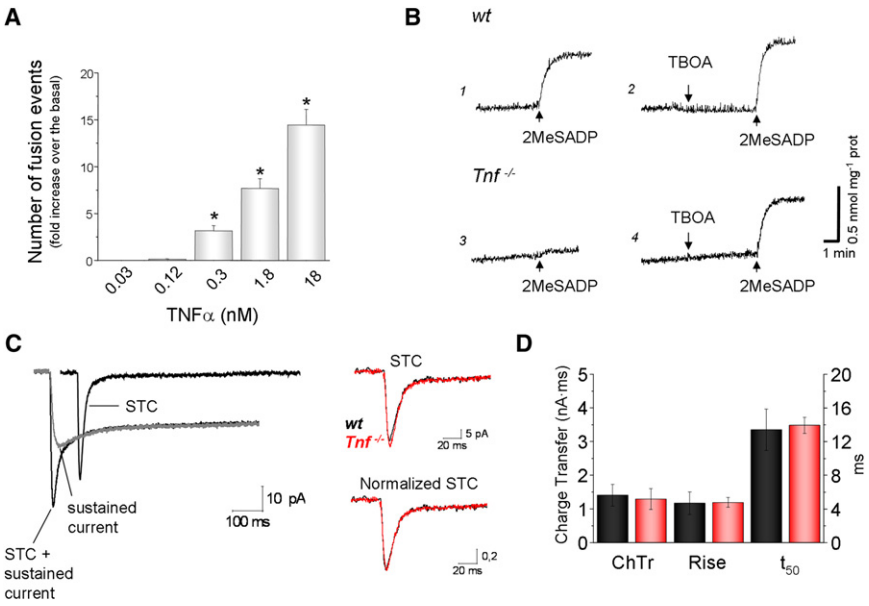

Figure 5. Constitutive Levels of TNFα Do Not Evoke Glutamate Exocytosis Directly, and Their Lack in *Tnf*$^{-/-}$ Astrocytes Does Not Reduce P2Y1R-Evoked Glutamate Release or Modify Synaptically Evoked Glutamate Transporter Currents

(A) Dose dependency of TNFα-evoked fusion events of VGLUT1-pHluorin-expressing vesicles in cultured astrocytes from *Tnf*$^{-/-}$ mice. Fusion events evoked by a 2 s pulse of TNFα (n = 3 for each concentration) were counted during an 8 s period starting at the start of the stimulus. Each individual histogram represents the mean number of fusion events expressed as % over the number of fusion events in basal condition, i.e., in the 8 s preceding the stimulus (66 ± 3.44; n = 15). *p < 0.05, paired t test versus basal. Notice that at 30 or 120 pM, i.e., at the concentrations restoring P2Y1R-evoked synaptic modulation and glutamatergic exocytosis, TNFα per se does not evoke exocytosis. A different set of experiments performed in WT astrocytes gave a similar result.

(B) P2Y1R-evoked glutamate release from cultures of *Tnf*$^{-/-}$ astrocytes is detected by the "GDH assay" in the presence, but not in the absence of the glutamate uptake blocker TBOA. (B1-B4) Fluorescence traces represent glutamate release in response to 2MeSADP (10 μM) detected in WT and *Tnf*$^{-/-}$ astrocytes in the absence (B1 and B3) and presence (B2 and B4) of TBOA (25 μM, about 5 min of incubation). In WT astrocytes, the 2MeSADP-evoked glutamate release detected in the absence and presence of TBOA is similar (n = 6 and n = 4, respectively; $p > 0.05$ unpaired t test). In contrast, in *Tnf*$^{-/-}$ astrocytes, the amount of 2MeSADP-evoked release detected in the absence of TBOA (n = 5) is significantly less than in its presence (n = 7; $p < 0.05$ unpaired t test). Notice that TBOA per se has no effects on the glutamate levels detected in the cultures.

(C) Left: synaptically evoked transporter current (STC). The representative trace is obtained by recording the current response to PP stimulation in a ML astrocyte and by subtracting to it a trace of the same current in the presence of the transporter antagonist TBOA (100μM, STC + sustained current). By blocking the transporter current, TBOA reveals a sustained component of the synaptically evoked current, reflecting a sustained potassium conductance (Diamond, 2005). Right: examples of raw and normalized STC recorded from WT and *Tnf*$^{-/-}$ astrocytes in situ shown for comparison of the kinetics. Each trace represents at least 5 averaged sweeps. Recordings are performed in the presence of Picrotoxin (100 μM) and NBQX (10 μM). Fiber volleys have been removed for clarity and were within the same range for WT and *Tnf*$^{-/-}$.

(D) Histograms showing the average values of: charge transfer (ChTr), 10–90 rise time (Rise) and decay time t_{50} of STCs in WT (black, n = 7) and *Tnf*$^{-/-}$ (red, n = 7) mice. Error bars are SEM.

up to levels comparable to those measured from WT astrocytes. In contrast, release in WT cultures did not vary significantly in the absence or presence of the uptake blocker (without TBOA: 0.60 ± 0.12; with TBOA: 0.78 ± 0.16 nmol/mg prot; n = 6 and 4; n.s., unpaired t test). The most logical explanation for these observations is that, in *Tnf*$^{-/-}$ astrocytes with defective exocytosis, P2Y1R stimulation induces much less glutamate release/time unit than in WT astrocytes, which favors more rapid scavenging of the released amino acid by glutamate transporters. As a consequence, less glutamate becomes available to GDH, which binds the amino acid with lower affinity than the transporters (Plaitakis and Zaganas, 2001), resulting in a reduced detection of release. Importantly, we previously reported a similar strong reduction of P2Y1R-evoked glutamate release in hippocampal *Tnf*$^{-/-}$ slices (Domercq et al., 2006). Therefore, the same problem, competition of defective release by uptake, could also occur in situ and ultimately prevent activation of pre-NMDAR. Alternatively, uptake efficiency could increase in *Tnf*$^{-/-}$ preparations, producing the same final result. To verify this latter possibility we studied synaptically evoked transporter currents (STCs) in situ (Diamond, 2005). We stimulated PP afferents and recorded STCs from whole-cell patch-clamped astrocytes in the dentate ML (Figure 5C; see Experimental Procedures). By comparing recordings in WT and *Tnf*$^{-/-}$ slices, we failed to find differences in any of the parameters analyzed (total charge transfer, currents' rise-time and t_{50}, Figures 5C and 5D). Therefore, in the absence of TNFα, ML astrocytes maintain the same number of functional glutamate transporters and take up the same amount of glutamate as in WT preparations, excluding astrocytic glutamate uptake as direct target of the TNFα-dependent control of gliotransmission.

Limiting Glutamate Uptake Restores Synaptic Efficacy of Gliotransmission in the Absence of TNFα

If P2Y1R stimulation fails to increase mEPSC frequency at GC synapses in *Tnf*$^{-/-}$ slices because of competition between defective astrocyte glutamate release and uptake, then blockade of the latter could be compensatory and artificially restore the synaptic effect lost by the defective release and, thereby, unmask its occurrence. To directly test this possibility, we added TBOA to hippocampal slices from *Tnf*$^{-/-}$ mice. At first, we checked the effects of the uptake blocker on basal activity in GCs. When applied at a subsaturating concentration (25 μM) (Brasier and Feldman, 2008), TBOA produced a clear change in

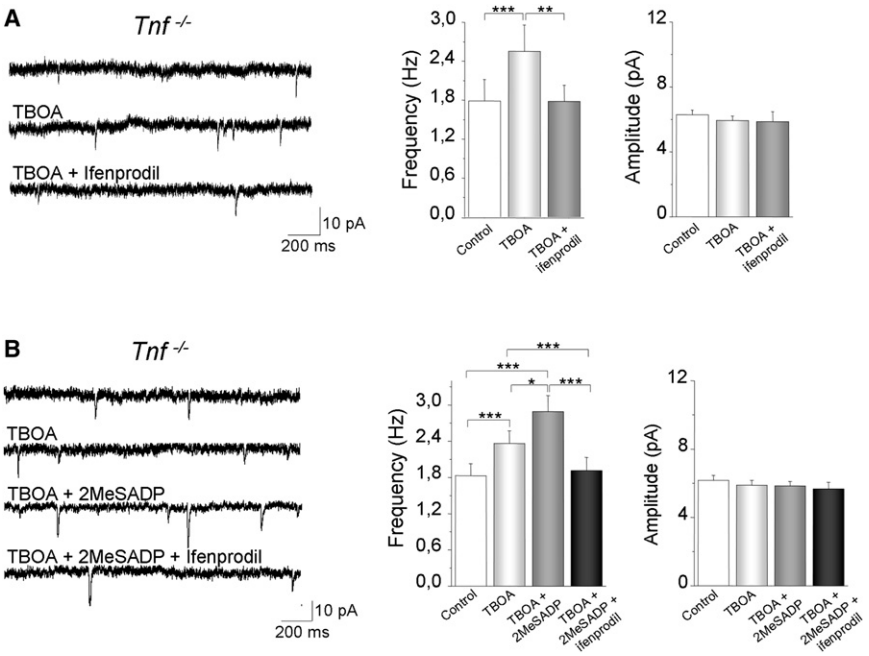

Figure 6. TBOA Reveals Synaptically Ineffective Glutamate Release from *Tnf*$^{-/-}$ Astrocytes In Situ

(A) Left: mEPSC activity recorded from a GC in a slice from a *Tnf*$^{-/-}$ mouse. Bath application of TBOA (25 μM) increases the events' frequency. Within 15 min the TBOA effect reaches steady state, but addition of the NR2B-selective NMDAR blocker ifenprodil (3 μM) fully counteracts it. Right: histograms show mean mEPSC frequency and amplitude in 10 GCs in the control period (control), during TBOA application (TBOA) and upon blocking NR2B-containing NMDAR (TBOA + ifenprodil). (B) Left: representative mEPSC traces in a *Tnf*$^{-/-}$ GC comparing the effect of subsequent additions of 25 μM TBOA (TBOA), 10 μM 2MeSADP in the presence of TBOA (TBOA + 2MeSADP) and 3 μM ifenprodil in the presence of the two former agents (TBOA + 2MeSADP + ifenprodil). Right: mEPSC mean frequency increases upon TBOA application; subsequent 2MeSADP stimulation produces a further significant increase, and addition of ifenprodil counteracts both effects, bringing the frequency back to control level. None of the treatments affected mEPSC amplitude (n = 18 GCs). The effect of 2MeSADP in presence of TBOA was observed in 10/18 *Tnf*$^{-/-}$ GCs (+47% ± 9%, $p < 0.001$). ***$p < 0.001$, **$p < 0.01$, *$p < 0.05$, one-way ANOVA + Scheffé test for multiple comparisons. Error bars: SEM.

mEPSC activity, with no other detectable effect on membrane currents (which were instead affected using 100 μM of the uptake blocker, data not shown). Notably, TBOA selectively increased the frequency of mEPSC events (+52% ± 13%; $p < 0.001$, n = 10 cells; Figure 6A), without changing their amplitude and kinetics. This effect was fully reversed by ifenprodil (Figure 6A), indicating that enhanced ambient glutamate activates pre-NMDAR. We then tested the effect of P2Y1R stimulation in the presence of the uptake blocker. Despite the TBOA-induced enhancement of basal mEPSC frequency in GCs, subsequent application of 2MeSADP in the continued presence of TBOA, produced a further significant increase in frequency (+47% ± 9%; $p < 0.001$; n = 18 cells) without changing amplitude of the miniature events (Figure 6B). Blocking NMDA receptors with ifenprodil in the presence of both 2MeSADP and TBOA fully reversed the overall increase in mEPSC frequency produced by the two agents (Figure 6B). These data indicate that, in *Tnf*$^{-/-}$ mice, inhibition of glutamate uptake by TBOA produces two effects on mEPSC frequency in GCs, both mediated by activation of presynaptic NR2B-containing NMDARs: (1) an increase in the basal frequency of the events and (2) a further 2MeSADP-dependent increase, resembling the effect produced by the P2Y1R agonist in WT mice. Taking all our data together, the most plausible explanation for the latter effect is that, in situ like in culture, astrocytic glutamate release is deregulated in the absence of TNFα. Thus, although astrocytic glutamate in *Tnf*$^{-/-}$ slices fails to induce pre-NMDAR-dependent modulation, reappearance of this type of effect in the presence of TBOA confirms that the transmitter is indeed released upon P2Y1R stimulation, but defectively and, because of competing uptake, it does not reach an extracellular concentration sufficient to activate pre-NMDAR.

DISCUSSION

TNFα Dependency of Gliotransmission

Here, we show that the neuromodulatory action of astrocytes at dentate GC synapses, via Ca^{2+}-dependent glutamate release and pre-NMDAR activation, is controlled by TNFα, i.e., that constitutive levels of the cytokine, estimated to be in the low picomolar range, need to be present for the neuromodulation to occur. TNFα controls steps in the stimulus-secretion coupling mechanism in astrocytes downstream of GPCR-evoked $[Ca^{2+}]_i$ elevations. In particular, we identified, in cultured astrocytes from *Tnf*$^{-/-}$ mice, a defect in the functional docking of glutamatergic vesicles, which decreases their readiness to fuse and dramatically slows down the kinetics of evoked exocytosis. As a consequence, slowly released glutamate is more rapidly taken up by competing uptake. This type of defect plausibly explains why astrocyte glutamate release fails to activate pre-NMDAR and loses synaptic efficacy in *Tnf*$^{-/-}$ slices and why use of low concentrations of the uptake blocker TBOA in this preparation can be compensatory and "restore" the neuromodulatory effect (Figure 7).

Levels of Activity Triggering Modulatory Gliotransmission at PP-GC Synapses

In the present study, we triggered gliotransmission by stimulation of P2Y1R, a native GPCR, with a pharmacological agonist, 2MeSADP, and used mEPSC activity as a readout of the evoked

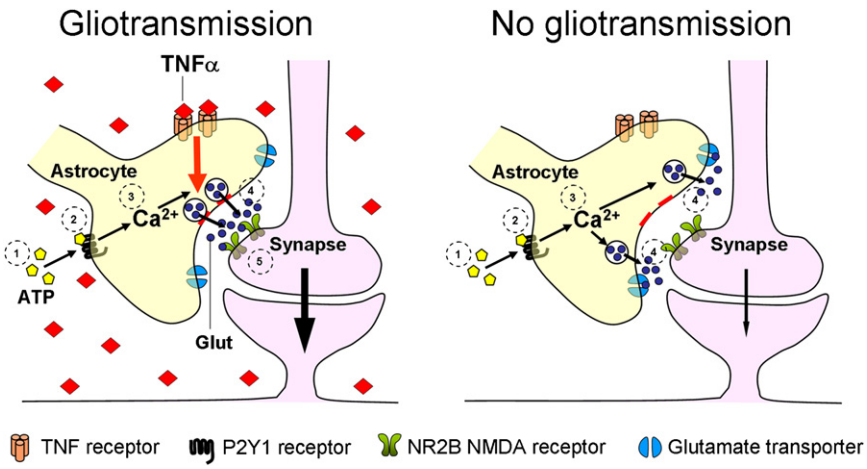

Figure 7. Schematic Summary of the TNFα Control on Gliotransmission at PP-GC Synapses in the Hippocampal Dentate Gyrus

Left: in the presence of constitutive TNFα (red diamonds), astrocyte vesicles containing glutamate (Glut., blue dots) are functionally docked at putative active zones on the plasma membrane of a perisynaptic astrocytic process. When ATP (yellow pentangles) is released (1) from GC synapses or the astrocytes (Jourdain et al., 2007), it activates P2Y1 receptors (2) and causes Ca^{2+} release from the internal stores in the astrocyte microcompartment (3). This in turn triggers fusion of the astrocyte vesicles in proximity of presynaptic NR2B containing NMDARs (4), eventually causing an increase in excitatory synaptic activity (5). Right: in the absence of TNFα, astrocytic glutamatergic vesicles are not correctly docked and ready to fuse. Therefore, when ATP triggers the usual signal-transduction in astrocytes, glutamate release occurs slowly and asynchronously and is scavenged by glutamate transporters before reaching pre-NMDA receptors to induce synaptic modulation.

neuromodulatory effect (that this is via astrocytic Ca^{2+} signaling was confirmed by sensitivity of neuromodulation to the Ca^{2+} buffer BAPTA introduced exclusively into astrocytes). This experimental paradigm was selected for two main reasons: because it induces neuromodulation in a highly reproducible manner, well adapted to study the role of TNFα, and because in these conditions, i.e., blocking action potentials, the P2Y1R-dependent pathway is not endogenously activated, which would have complicated interpretation of the results. Indeed, P2Y1R-dependent gliotransmission at PP-GC synapses is a physiological modulatory mechanism triggered in response to action potential-dependent synaptic transmission (Jourdain et al., 2007) but not to action potential-independent, spontaneous synaptic release events. The evidence for this comes from the observation that blocking the P2Y1R-dependent pathway at different levels (P2Y1R, astrocyte $[Ca^{2+}]_i$ elevation, pre-NMDAR), led, in all cases, to a reduction in basal EPSC frequency when the synaptic activity was recorded in the absence of TTX (sEPSC; Jourdain et al., 2007). In contrast, no effect was produced if TTX was present and action potentials were abolished (mEPSC; Figure 1). In keeping, the absence of TNFα in *Tnf*$^{-/-}$ slices or in WT slices incubated with sTNFR, while abolishing 2MeSADP-evoked neuromodulation, did not produce any change in basal mEPSC frequency. Intriguingly, we recently observed that action potentials in the hippocampal dentate gyrus synchronize several small (~1 μm) "Ca^{2+} microdomains" in astrocytic processes (most likely representing the random local responses to single synapse release events) and produce stronger and spatially larger (several μm) $[Ca^{2+}]_i$ elevations, in part mediated by P2Y1R (Chuquet et al., 2010). This latter, action potential-evoked Ca^{2+} activity, not the former, is associated to the neuromodulatory response of the astrocyte. Therefore, it seems key for physiological astrocyte synaptic modulation to occur, that not just individual "Ca^{2+} microdomains" but larger process segments are synchronously active, most likely to release glutamate in sufficient amounts to activate nearby pre-NMDAR. Hence, we can hypothesize that synchronous $[Ca^{2+}]_i$ increase in large domains of the astrocyte process leads to synchronous glutamate release from different release sites.

Kinetic Requirements of Glutamate Release from Astrocytes: The Role of TNFα

Overall, our data suggest that when constitutive TNFα is removed P2Y1R-evoked gliotransmission loses its synaptic efficacy because of a loss of synchronicity, not at the level of $[Ca^{2+}]_i$ elevations, but at the ensuing glutamate release process. The mechanistic studies in cultured astrocytes, where P2Y1R stimulation induces exocytosis of glutamatergic vesicles (Bowser and Khakh, 2007; Domercq et al., 2006), point to a specific role of the cytokine in promoting functional docking of the vesicles at release sites and, consequently, in permitting their immediate fusion upon stimulation. A characteristic of GPCR-evoked exocytosis in vitro is that release-ready vesicles (those "residents" in the TIRF field) undergo fusion rapidly (peak at ~300 ms) and in a highly synchronous manner (Bergami et al., 2008; Bezzi et al., 2004; Domercq et al., 2006; Marchaland et al., 2008). However, when constitutive TNFα is missing, all vesicles, including the "resident" ones, are not ready to fuse immediately upon stimulation. Ultimately, they do fuse, but randomly in time (small peak at ~4 s) and over a much longer period than when the cytokine is present. Interestingly, these functional defects are reminiscent of those reported in neurosecretory cells upon interfering with the molecular machinery promoting vesicle docking (reviewed in Verhage and Sørensen, 2008).

Could altered vesicular exocytosis, as observed in cultured *Tnf*$^{-/-}$ astrocytes, underlie the defect of glutamate release observed in situ? Although no conclusive evidence exists yet, we previously reported that the process in situ is sensitive to exocytosis blockers (Domercq et al., 2006; Jourdain et al., 2007). Moreover, we showed that VGLUT-expressing synaptic-like microvesicles (SLMV) are present in the perisynaptic processes of astrocytes in the dentate ML (Bezzi et al., 2004), mostly laying in proximity (<150 nm) of NR2B subunits signaling pre-NMDAR in adjacent excitatory nerve terminals (Jourdain et al., 2007). Based on this information, we could

hypothesize that pre-NMDAR activation requires glutamate released by the fusion of more than one such astrocytic vesicle, which would explain why loss of synchronicity in the exocytosis of glutamatergic vesicles critically affects the activation state of NMDAR.

Gliotransmission Is Not Controlled Only by GPCR-Evoked $[Ca^{2+}]_i$ Elevations

An intriguing observation of the present study is that TNFα, while exerting a tight control on astrocyte glutamate release, does not influence upstream GPCR-mediated $[Ca^{2+}]_i$ elevations, notably those directly relevant to the release process and to neuromodulation. Thus, by using short focal 2MeSADP applications, we succeeded in inducing local $[Ca^{2+}]_i$ rises in astrocytic processes with spatial-temporal characteristics reproducing the P2Y1R-dependent Ca^{2+} signals evoked by endogenous synaptic activity and involved in its modulation (Chuquet et al., 2010). These 2MeSADP-induced local Ca^{2+} signals were in all similar in WT and in *Tnf*$^{-/-}$ slices, although in the latter local or even bath application of the P2Y1R agonist did not produce any synaptic modulation. In keeping, fast submembrane $[Ca^{2+}]_i$ elevations evoked by 2MeSADP in cultured astrocytes, which correlate in space and time to exocytic fusions of glutamatergic vesicles (Marchaland et al., 2008), were identical in WT and *Tnf*$^{-/-}$ astrocytes, although in the latter cells, P2Y1R-evoked vesicle fusions and glutamate release were dramatically altered. Therefore, our data demonstrate that the induction of $[Ca^{2+}]_i$ elevation in astrocytes, even when produced by stimulation of the appropriate GPCR, is not "necessary and sufficient" for functional gliotransmission to occur (Araque et al., 1998) if a downstream control mechanism is altered. Thus, we identify the existence of permissive/homeostatic factors like TNFα that control stimulus-secretion coupling in astrocytes and its synaptic effects independently of, and in addition to, $[Ca^{2+}]_i$ elevations. We believe that this finding represents a relevant contribution to the understanding of the process of gliotransmission, particularly in view of recent conflicting results. Indeed, parallel investigations using different experimental paradigms succeeded or failed in detecting an astrocytic control on synaptic transmission and plasticity (Agulhon et al., 2010; Fellin et al., 2004; Fiacco et al., 2007; Henneberger et al., 2010; Perea and Araque, 2007). While the present debate focuses on the required characteristics of astrocytic $[Ca^{2+}]_i$ elevations for the control to occur (Hamilton and Attwell, 2010; Kirchhoff, 2010), our findings call for attention also to the role of additional factors.

TNFα Controls Excitatory Transmission: Dose Dependency, Pre- and Postsynaptic Targets

Our study reveals a complexity and dose dependency of the TNFα effects on astrocyte glutamate release and on mEPSC activity in general. The effects on P2Y1R- or CXCR4-evoked glutamate release observed in the present study, which affect presynaptic excitatory function, depend on the presence of constitutive TNFα and are "reconstituted" in *Tnf*$^{-/-}$ astrocytes by adding low picomolar concentrations of the cytokine. However, in line with our previous observations (Bezzi et al., 1998; Bezzi et al., 2001), at higher (nanomolar) concentrations, the cytokine induces exocytosis of glutamatergic vesicles directly, suggesting that its impact on excitatory transmission may change at these concentrations (see below).

Incubation of *Tnf*$^{-/-}$ slices with low picomolar levels of TNFα has an additional effect on the amplitude of mEPSC events, which is slightly but significantly increased by the presence of the cytokine. This effect, independent of astrocyte P2Y1R-dependent glutamate signaling, is reminiscent of the effect mediating synaptic scaling in WT mice via surface insertion of postsynaptic AMPAR subunits (Stellwagen and Malenka, 2006). This observation suggests that TNFα exerts multiple, possibly coordinated, regulatory actions at excitatory synapses, which apparently converge in strengthening synaptic connectivity. Intriguingly, we did not find that basal mEPSC amplitude was reduced in *Tnf*$^{-/-}$ slices compared to WT slices (see also Beattie et al., 2002; Kaneko et al., 2008; Stellwagen and Malenka, 2006). This is probably because TNFα mediates exclusively the scaling-up of synapses, a phenomenon in which synapses adapt to increased TNFα levels, whereas the opposite scaling-down phenomenon might be controlled by TNFα-independent mechanisms (Aizenman and Pratt, 2008; Cingolani et al., 2008).

Relevance of the TNFα-Dependent Control of the Astrocytic Input to Excitatory Synapses

Our study introduces the concept of regulation of the astrocytic input to synapses by ambient factors like TNFα. This is particularly relevant also because we show that the cytokine displays concentration-dependent effects on astrocytic glutamate release, going from a permissive/gating action to direct stimulation. We do not know if these represent mechanistically distinct modes of action or, perhaps more probably, a gradual shift in the effects of TNFα. In the latter case, we could hypothesize that, even at gating levels, small fluctuations in TNFα concentrations, could subtly modify the astrocytic input to synapses. Physiological processes like sleep have been proposed to be regulated by local variations in TNFα levels in the brain related to the sleep-wake cycle, and sleep deregulation can be induced by injections of the cytokine (Imeri and Opp, 2009; Krueger, 2008). Therefore, an intriguing hypothesis is that the TNFα control of gliotransmission is involved in sleep homeostasis together with other glial pathways already identified (Fellin et al., 2009; Halassa et al., 2009). Moreover, the levels of TNFα are subject to dramatic changes in pathological conditions when microglia releases large amounts of the cytokine. We have already shown in a cell culture model that in such a situation, TNFα strongly amplifies glutamate release from astrocytes (Bezzi et al., 2001). We can then hypothesize that a pathology-induced switch in the TNFα levels may have an important impact on the astrocytic input to synapses, notably in the presynaptic regulation of neuronal activity in the PP-GC hippocampal synaptic circuit. This may perturb the normal control by this circuit on critical processes such as memory formation and physiological limbic system excitability.

EXPERIMENTAL PROCEDURES

TNFα-Deficient Mice

Mice homozygous for the null mutant TNFα (*Tnf*$^{-/-}$) allele were generated and maintained on a C57BL/6J background as described in the original study

(Pasparakis et al., 1996). Knockout animals were housed under specific pathogen-free conditions together with age- and sex-matched WT mice.

Hemibrain Slices

Hemibrain horizontal slices (400 μm) containing intact perforant path afferents (Staley and Mody, 1991) were obtained from 18- to 23-day-old C57/BL6 male and female WT and *Tnf*$^{-/-}$ mice and maintained in 95% O_2 and 5% CO_2-gassed artificial cerebrospinal fluid (ACSF), containing (in mM): 118 NaCl, 2 KCl, 2 $MgCl_2$, 2.5 $CaCl_2$, 25 $NaHCO_3$, 1.2 NaH_2PO_4, 10 glucose, and 0.1 picrotoxin at pH 7.4. In some experiments astrocytes were loaded with sulphorhodamine 101 (SR-101, 5μM) by incubating the slices at 37°C with the dye for 15 min.

Patch-Clamp Recordings

Details are provided in the Supplemental Experimental Procedures.

Currents Analysis

Currents have been analyzed essentially as reported in Jourdain et al. (2007); see Supplemental Experimental Procedures.

Astrocyte Cultures and TIRF Imaging Experiments

Astrocyte cultures were obtained from WT and *Tnf*$^{-/-}$ newborn mice and prepared essentially as described (Bezzi et al., 2001; Domercq et al., 2006); TIRF imaging experiments were performed essentially as described (Marchaland et al., 2008); see Supplemental Experimental Procedures.

Two-Photon Ca^{2+} Imaging In Situ

In situ Ca^{2+} imaging experiments in single astrocytes were performed using a Prairie Technology Ultima (Madison, WI) two-photon laser scanning microscope consisting of an Olympus BX61WI with a Prairie galvanometer scanning system and a 60× water immersion objective lens (numerical aperture: 0.9; Olympus Optical LUMPlan FI/IR). Fluorescence emission was directed by a 700 longpass dichroic mirror (LPDM), divided with a 575 LPDM into green and red channels and further restricted with 607/45 nm and 525/70 nm filters placed before the green and red photomultiplier, respectively. "Dodt contrast" images were generated by spatially filtering the forward scattered IR laser light with a Dodt tube and detected by an additional photomultiplier tube. The light source was a pulsed laser (Chameleon-XR, Coherent, Santa Clara, CA) tuned to 815 nm for calcium and "Dodt contrast" imaging and 890 nm for the sole morphology acquisition with TxR fluorescence. Crop of the image at the region of interest allowed both high spatial (5 pixels/μm) and temporal (frame rate, 10–17 Hz) resolution in frame scan mode (dwell time, 2.4 μs). Using these conditions, the laser power could be limited to 9–13 mW (measured before the objective) to minimize the potential effect of illumination on $[Ca^{2+}]_i$ as reveled by no change of Fluo-4 fluorescence between the first and the last 10 s of the imaging sequence. Focal and short 2MeSADP puffs (5 ms, 10 μM) to detect local $[Ca^{2+}]_i$ elevations were delivered by low-pressure ejection (4 psi) via a PV830 Pneumatic PicoPump (WPI). By simultaneous acquisition of florescence and high-contrast transmitted-light imaging (Dodt contrast) we were able to position the ejection pipette within 3–8 μm from the imaged astrocyte process, paying attention to not enter in the arbor of the patched astrocyte. In some experiments, we verified the spatial diffusion of the drug (~10–15 μm diameter) including TxR in the ejection pipette. All solutions contained TTX 1 μM and Picrotoxin 100 μM.

Image Analysis

The structure of the process was extracted from the rest of the image (red channel, TxR fluorescence) by a segmentation paradigm combining tools of mathematical morphology implemented in Matlab. The process was then subdivided in many contiguous subregions (SRs, 5–16 μm^2), roughly corresponding to the spatial extent of the $[Ca^{2+}]_i$ elevation evoked by a local 2MeSADP puff. The amplitude of $[Ca^{2+}]_i$ transients was measured in the selected responding SR by dividing the Ca^{2+} signal by the TxR signal in order to correct possible transient z motion. Events' duration was calculated as the time-interval between the point at which the transient reached 50% of its maximal amplitude and the point at which it declined back to 50% (full width at half maximum [FWHM]). Rise-time was calculated from 10% to 90% of the peak amplitude. In the few cases when the $[Ca^{2+}]_i$ elevation invaded more than one SR, kinetics of the event were calculated on the first responding SR. Recordings showing any drift (x, y, or z) were discarded. Traces were subjected to median filter before analysis.

Other Imaging Experiments In Situ

In a set of electrophysiological experiments in hippocampal slices, BAPTA was dialyzed into the astrocytes. To indirectly follow the process, we monitored diffusion of a fluorescent dye, Alexa 488 hydrazide or Alexa 594, from the whole-cell patched astrocyte to the astrocytic syncytium in the dentate ML. Within 15–30 min tens of gap junction-coupled astrocytes were labeled by the dye (Shigetomi et al., 2008). After removal of the pipette, florescence in the syncytium remained stable for at least 1 hr and during the whole experiment. Images were normally observed on an Olympus BX51WI microscope (20× water-immersion objective). The excitation light beam (488 nm/590 nm, monochromator, Visichrome, Visitron; controlled by Metafluor software, Universal Imaging) was introduced through the objective by a long-pass filter (Olympus U-N31001); fluorescence emission was collected (cooled CCD camera, CoolSNAP-HQ, Roper Scientific) with a 1 frame/s acquisition rate. Some of the experiments (Figures 1A–1D) were performed under a two-photon laser scanning microscope with a 40× water-immersion objective. For in situ visualization of astrocytes and granule cells loaded respectively with SR-101 and Alexa 488, or Alexa 594 and Alexa 488, excitation was provided at 800–830 nm.

Enzymatic Assay of Endogenous Glutamate Release

Efflux of endogenous glutamate from cell cultures was monitored in continuous by use of an enzymatic assay as previously described (Bezzi et al., 1998); see Supplemental Experimental Procedures.

SUPPLEMENTAL INFORMATION

Supplemental Information includes three figures and Supplemental Experimental Procedures and can be found with this article online at doi:10.1016/j.neuron.2011.02.003.

ACKNOWLEDGMENTS

We thank R.H. Edwards and S. Voglmaier for providing VGLUT1pHluorin and VGLUT1mCherry constructs, N. Liaudet for developing the custom-made program for two-photon Ca^{2+} imaging analysis, H. Stubbe, C. Calì, J. Marchaland, P. Spagnuolo, and J. Gremion for help on experiments on cultured astrocytes, and C. Duerst and M. Saxena for help with electrophysiology experiments. We also thank A. Scimemi for precious help and suggestions on STC recordings. This work was supported by grants from the Swiss National Foundation (3100A0-100850, 3100A0-120398, and NCCR Transcure) to A.V. and from the University of Lausanne, grant FBM 2006, and Novartis Foundation (26077772) to P.B. M.S. is recipient of a University of Lausanne FBM PhD fellowship.

Accepted: December 22, 2010
Published: March 9, 2011

REFERENCES

Agulhon, C., Fiacco, T.A., and McCarthy, K.D. (2010). Hippocampal short- and long-term plasticity are not modulated by astrocyte Ca^{2+} signaling. Science *327*, 1250–1254.

Aizenman, C.D., and Pratt, K.G. (2008). There's more than one way to scale a synapse. Neuron *58*, 651–653.

Araque, A., Sanzgiri, R.P., Parpura, V., and Haydon, P.G. (1998). Calcium elevation in astrocytes causes an NMDA receptor-dependent increase in the frequency of miniature synaptic currents in cultured hippocampal neurons. J. Neurosci. *18*, 6822–6829.

Bains, J.S., and Oliet, S.H. (2007). Glia: They make your memories stick!. Trends Neurosci. *30*, 417–424.

Balaji, J., and Ryan, T.A. (2007). Single-vesicle imaging reveals that synaptic vesicle exocytosis and endocytosis are coupled by a single stochastic mode. Proc. Natl. Acad. Sci. USA *104*, 20576–20581.

Beattie, E.C., Stellwagen, D., Morishita, W., Bresnahan, J.C., Ha, B.K., Von Zastrow, M., Beattie, M.S., and Malenka, R.C. (2002). Control of synaptic strength by glial TNFalpha. Science *295*, 2282–2285.

Bergami, M., Santi, S., Formaggio, E., Cagnoli, C., Verderio, C., Blum, R., Berninger, B., Matteoli, M., and Canossa, M. (2008). Uptake and recycling of pro-BDNF for transmitter-induced secretion by cortical astrocytes. J. Cell Biol. *183*, 213–221.

Bezzi, P., Carmignoto, G., Pasti, L., Vesce, S., Rossi, D., Rizzini, B.L., Pozzan, T., and Volterra, A. (1998). Prostaglandins stimulate calcium-dependent glutamate release in astrocytes. Nature *391*, 281–285.

Bezzi, P., Domercq, M., Brambilla, L., Galli, R., Schols, D., De Clercq, E., Vescovi, A., Bagetta, G., Kollias, G., Meldolesi, J., and Volterra, A. (2001). CXCR4-activated astrocyte glutamate release via TNFalpha: Amplification by microglia triggers neurotoxicity. Nat. Neurosci. *4*, 702–710.

Bezzi, P., Gundersen, V., Galbete, J.L., Seifert, G., Steinhäuser, C., Pilati, E., and Volterra, A. (2004). Astrocytes contain a vesicular compartment that is competent for regulated exocytosis of glutamate. Nat. Neurosci. *7*, 613–620.

Boulanger, L.M. (2009). Immune proteins in brain development and synaptic plasticity. Neuron *64*, 93–109.

Bowser, D.N., and Khakh, B.S. (2007). Two forms of single-vesicle astrocyte exocytosis imaged with total internal reflection fluorescence microscopy. Proc. Natl. Acad. Sci. USA *104*, 4212–4217.

Brasier, D.J., and Feldman, D.E. (2008). Synapse-specific expression of functional presynaptic NMDA receptors in rat somatosensory cortex. J. Neurosci. *28*, 2199–2211.

Calì, C., Marchaland, J., Regazzi, R., and Bezzi, P. (2008). SDF 1-alpha (CXCL12) triggers glutamate exocytosis from astrocytes on a millisecond time scale: Imaging analysis at the single-vesicle level with TIRF microscopy. J. Neuroimmunol. *198*, 82–91.

Chuquet, J., Bhaukaurally, K., Santello, M., Liaudet, N., Bouvier, D., Di Castro, A., and Volterra, A. (2010). Fast and local calcium transients in astrocyte processes encode synaptic activity in the adult hippocampus. FENS Abstr. *5*, 044.4.

Cingolani, L.A., Thalhammer, A., Yu, L.M., Catalano, M., Ramos, T., Colicos, M.A., and Goda, Y. (2008). Activity-dependent regulation of synaptic AMPA receptor composition and abundance by beta3 integrins. Neuron *58*, 749–762.

Corlew, R., Brasier, D.J., Feldman, D.E., and Philpot, B.D. (2008). Presynaptic NMDA receptors: newly appreciated roles in cortical synaptic function and plasticity. Neuroscientist *14*, 609–625.

Diamond, J.S. (2005). Deriving the glutamate clearance time course from transporter currents in CA1 hippocampal astrocytes: Transmitter uptake gets faster during development. J. Neurosci. *25*, 2906–2916.

Domercq, M., Brambilla, L., Pilati, E., Marchaland, J., Volterra, A., and Bezzi, P. (2006). P2Y1 receptor-evoked glutamate exocytosis from astrocytes: control by tumor necrosis factor-alpha and prostaglandins. J. Biol. Chem. *281*, 30684–30696.

Fellin, T., Pascual, O., Gobbo, S., Pozzan, T., Haydon, P.G., and Carmignoto, G. (2004). Neuronal synchrony mediated by astrocytic glutamate through activation of extrasynaptic NMDA receptors. Neuron *43*, 729–743.

Fellin, T., Halassa, M.M., Terunuma, M., Succol, F., Takano, H., Frank, M., Moss, S.J., and Haydon, P.G. (2009). Endogenous nonneuronal modulators of synaptic transmission control cortical slow oscillations in vivo. Proc. Natl. Acad. Sci. USA *106*, 15037–15042.

Fiacco, T.A., Agulhon, C., Taves, S.R., Petravicz, J., Casper, K.B., Dong, X., Chen, J., and McCarthy, K.D. (2007). Selective stimulation of astrocyte calcium in situ does not affect neuronal excitatory synaptic activity. Neuron *54*, 611–626.

Gosselin, D., and Rivest, S. (2007). Role of IL-1 and TNF in the brain: Twenty years of progress on a Dr. Jekyll/Mr. Hyde duality of the innate immune system. Brain Behav. Immun. *21*, 281–289.

Halassa, M.M., Florian, C., Fellin, T., Munoz, J.R., Lee, S.Y., Abel, T., Haydon, P.G., and Frank, M.G. (2009). Astrocytic modulation of sleep homeostasis and cognitive consequences of sleep loss. Neuron *61*, 213–219.

Hamilton, N.B., and Attwell, D. (2010). Do astrocytes really exocytose neurotransmitters? Nat. Rev. Neurosci. *11*, 227–238.

Henneberger, C., Papouin, T., Oliet, S.H., and Rusakov, D.A. (2010). Long-term potentiation depends on release of D-serine from astrocytes. Nature *463*, 232–236.

Imeri, L., and Opp, M.R. (2009). How (and why) the immune system makes us sleep. Nat. Rev. Neurosci. *10*, 199–210.

Jourdain, P., Bergersen, L.H., Bhaukaurally, K., Bezzi, P., Santello, M., Domercq, M., Matute, C., Tonello, F., Gundersen, V., and Volterra, A. (2007). Glutamate exocytosis from astrocytes controls synaptic strength. Nat. Neurosci. *10*, 331–339.

Kaneko, M., Stellwagen, D., Malenka, R.C., and Stryker, M.P. (2008). Tumor necrosis factor-alpha mediates one component of competitive, experience-dependent plasticity in developing visual cortex. Neuron *58*, 673–680.

Kirchhoff, F. (2010). Neuroscience. Questionable calcium. Science *327*, 1212–1213.

Krueger, J.M. (2008). The role of cytokines in sleep regulation. Curr. Pharm. Des. *14*, 3408–3416.

Marchaland, J., Calì, C., Voglmaier, S.M., Li, H., Regazzi, R., Edwards, R.H., and Bezzi, P. (2008). Fast subplasma membrane Ca^{2+} transients control exo-endocytosis of synaptic-like microvesicles in astrocytes. J. Neurosci. *28*, 9122–9132.

Nicholls, D.G., Sihra, T.S., and Sanchez-Prieto, J. (1987). Calcium-dependent and -independent release of glutamate from synaptosomes monitored by continuous fluorometry. J. Neurochem. *49*, 50–57.

Ohara-Imaizumi, M., Fujiwara, T., Nakamichi, Y., Okamura, T., Akimoto, Y., Kawai, J., Matsushima, S., Kawakami, H., Watanabe, T., Akagawa, K., and Nagamatsu, S. (2007). Imaging analysis reveals mechanistic differences between first- and second-phase insulin exocytosis. J. Cell Biol. *177*, 695–705.

Pasparakis, M., Alexopoulou, L., Episkopou, V., and Kollias, G. (1996). Immune and inflammatory responses in TNF alpha-deficient mice: A critical requirement for TNF alpha in the formation of primary B cell follicles, follicular dendritic cell networks and germinal centers, and in the maturation of the humoral immune response. J. Exp. Med. *184*, 1397–1411.

Perea, G., and Araque, A. (2007). Astrocytes potentiate transmitter release at single hippocampal synapses. Science *317*, 1083–1086.

Perea, G., Navarrete, M., and Araque, A. (2009). Tripartite synapses: Astrocytes process and control synaptic information. Trends Neurosci. *32*, 421–431.

Petravicz, J., Fiacco, T.A., and McCarthy, K.D. (2008). Loss of IP3 receptor-dependent Ca^{2+} increases in hippocampal astrocytes does not affect baseline CA1 pyramidal neuron synaptic activity. J. Neurosci. *28*, 4967–4973.

Plaitakis, A., and Zaganas, I. (2001). Regulation of human glutamate dehydrogenases: Implications for glutamate, ammonia and energy metabolism in brain. J. Neurosci. Res. *66*, 899–908.

Rossi, D., Brambilla, L., Valori, C.F., Crugnola, A., Giaccone, G., Capobianco, R., Mangieri, M., Kingston, A.E., Bloc, A., Bezzi, P., and Volterra, A. (2005). Defective tumor necrosis factor-alpha-dependent control of astrocyte glutamate release in a transgenic mouse model of Alzheimer disease. J. Biol. Chem. *280*, 42088–42096.

Shigetomi, E., Bowser, D.N., Sofroniew, M.V., and Khakh, B.S. (2008). Two forms of astrocyte calcium excitability have distinct effects on NMDA receptor-mediated slow inward currents in pyramidal neurons. J. Neurosci. *28*, 6659–6663.

Shigetomi, E., Kracun, S., Sofroniew, M.V., and Khakh, B.S. (2010). A genetically targeted optical sensor to monitor calcium signals in astrocyte processes. Nat. Neurosci. *13*, 759–766.

Staley, K.J., and Mody, I. (1991). Integrity of perforant path fibers and the frequency of action potential independent excitatory and inhibitory synaptic events in dentate gyrus granule cells. Synapse *9*, 219–224.

Stellwagen, D., and Malenka, R.C. (2006). Synaptic scaling mediated by glial TNF-alpha. Nature *440*, 1054–1059.

Stellwagen, D., Beattie, E.C., Seo, J.Y., and Malenka, R.C. (2005). Differential regulation of AMPA receptor and GABA receptor trafficking by tumor necrosis factor-alpha. J. Neurosci. *25*, 3219–3228.

Toonen, R.F., Kochubey, O., de Wit, H., Gulyas-Kovacs, A., Konijnenburg, B., Sørensen, J.B., Klingauf, J., and Verhage, M. (2006). Dissecting docking and tethering of secretory vesicles at the target membrane. EMBO J. *25*, 3725–3737.

Tritsch, N.X., and Bergles, D.E. (2007). Defining the role of astrocytes in neuromodulation. Neuron *54*, 497–500.

Turrigiano, G.G. (2008). The self-tuning neuron: Synaptic scaling of excitatory synapses. Cell *135*, 422–435.

Verhage, M., and Sørensen, J.B. (2008). Vesicle docking in regulated exocytosis. Traffic *9*, 1414–1424.

Vitkovic, L., Bockaert, J., and Jacque, C. (2000). "Inflammatory" cytokines: Neuromodulators in normal brain? J. Neurochem. *74*, 457–471.

Voglmaier, S.M., Kam, K., Yang, H., Fortin, D.L., Hua, Z., Nicoll, R.A., and Edwards, R.H. (2006). Distinct endocytic pathways control the rate and extent of synaptic vesicle protein recycling. Neuron *51*, 71–84.

Volterra, A., and Meldolesi, J. (2005). Astrocytes, from brain glue to communication elements: The revolution continues. Nat. Rev. Neurosci. *6*, 626–640.

Wetherington, J., Serrano, G., and Dingledine, R. (2008). Astrocytes in the epileptic brain. Neuron *58*, 168–178.

Zenisek, D., Steyer, J.A., and Almers, W. (2000). Transport, capture and exocytosis of single synaptic vesicles at active zones. Nature *406*, 849–854.